

Design and Performance Evaluation of a LoRa-Based Data Transmission System for Micro Smart Grid Devices in Water Quality Monitoring Stations

Jarun Khonrang¹, Pairoj Duangnakorn¹, Seksan Winyangkul¹, Thanapon Saengsuwan¹,
Suppat Rungrangsilp², Kamol Boonlom^{1*}

¹Faculty of Industrial Technology, Chiang Rai Rajabhat University, Chiang Rai 57100, Thailand

²School of Electronic and Electrical Engineering, University of Leeds, Leeds LS2 9JT, United Kingdom

*Corresponding author's email: kamolboonlom@gmail.com

Article info:

Received: 3 September 2025

Revised: 17 October 2025

Accepted: 10 January 2026

DOI:

[10.69650/rast.2026.263801](https://doi.org/10.69650/rast.2026.263801)

Keywords:

LoRa IoT Network
Micro Smart Grid
Water Quality Monitoring
Solar-Powered IoT
Groundwater Quality

ABSTRACT

This paper presents the design and evaluation of a LoRa-based Internet of Things (IoT) communication system for water quality monitoring integrated with a micro smart grid. The system operates at 923.2 MHz with 125 kHz bandwidth using the SX1276 transceiver and FHSS modulation to achieve long-range, low-power communication. A single-channel LoRa gateway, built on a Raspberry Pi 3, forwards sensor data to the ThingSpeak cloud platform through a LoRa Network and Application Server for real-time visualization of environmental and electrical parameters. Theoretical modeling with the Free-Space Path Loss (FSPL) model and Keysight ADS simulation predicted a received power of -72.8 dBm at 2 km. Field measurements recorded -108 dBm, showing an extra 35 dB attenuation from Fresnel obstruction, multipath, and ground reflection. Despite this, the system achieved a 95% packet delivery ratio (PDR) with a measured SNR of $+9$ dB, consistent with link budget analysis. With a 30-byte payload, the time-on-air was ~ 4.8 ms, yielding an effective throughput of 47.5 kbps. Results confirm the system's reliability, efficiency, and suitability for solar-powered monitoring stations, supporting smart grid and water management applications.

1. Introduction

The proliferation of Internet of Things (IoT) technologies has necessitated the development of communication networks capable of supporting extensive device connectivity with minimal energy and cost requirements. Low Power Wide Area Network (LPWAN) technologies have emerged as a fundamental component in this landscape, with LoRa (Long Range) technology gaining particular prominence. LoRa offers a distinctive combination of long-range communication, low power consumption, and scalability, characteristics that are highly advantageous for large-scale, geographically dispersed IoT deployments [2-3]. Its ability to maintain connectivity across challenging environments, coupled with its cost-effectiveness and adaptability, has positioned LoRa as a key enabler for a wide range of IoT applications, including environmental monitoring, agriculture, industrial automation, and urban infrastructure management [1], [12-14].

In the context of smart grid systems, the application of LoRa technology presents significant advantages for enhancing data transmission capabilities. Smart grids require robust, reliable, and scalable communication infrastructures to facilitate real-time data exchange between distributed assets [15-16], [20]. LoRa's long communication range, strong penetration through physical obstacles, and minimal energy demands make it particularly suitable for supporting the dense and geographically widespread sensor networks essential to smart grid operations (Giordano et al., 2018) [4], [6-7].

Moreover, the inherent low deployment and maintenance costs associated with LoRa networks contribute to economic efficiency, while its support for secure, low-bandwidth data transmission aligns well with the communication requirements of smart metering, grid monitoring, and demand-response applications (Hassan et al., 2019) [5], [17-18]. Consequently, the integration of LoRa technology within smart grid frameworks not only enhances operational resilience and efficiency but also supports broader objectives related to energy sustainability and grid modernization.

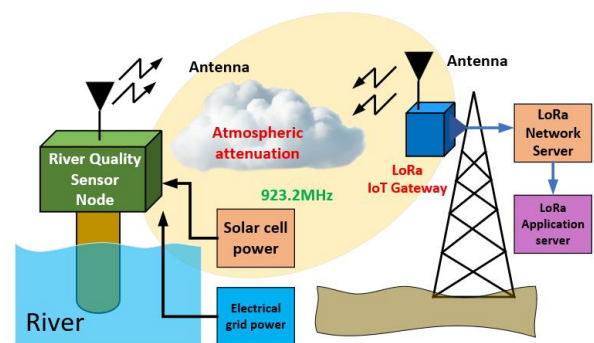


Fig. 1 Communication system used in this research.

Building upon these capabilities, this research focuses on the comprehensive design and implementation of a data transmission system tailored for micro smart grid devices. The system is specifically developed to support solar-powered water quality monitoring stations, which integrate both renewable energy sources and conventional electrical grid connections. The primary objective of this study is to design an energy-efficient and reliable communication infrastructure that facilitates real-time transmission of environmental and electrical parameters across remote and potentially infrastructure-limited areas.

A key component of the research involves the detailed analysis of the wireless communication channel, with a focus on characterizing the path loss behavior under varying environmental and deployment conditions. The study will conduct both theoretical and empirical evaluations, including link budget calculations, to estimate the expected signal strength, communication range, and overall link performance. The path loss models considered will account for various factors such as terrain, vegetation, antenna height, and urban interference, which are critical in rural and semi-urban deployment scenarios typical of water quality stations.

Experimental field measurements of the Received Signal Strength Indicator (RSSI) will be conducted at various distances and conditions to compare with the theoretical predictions. This comparison will enable the calibration of path loss models and help refine system parameters such as spreading factors, transmission power, and antenna configuration. In addition to RSSI, the system's packet delivery performance—measured in terms of Packet Delivery Ratio (PDR) and latency—will be assessed to evaluate the reliability and efficiency of the transmission system under real-world operating conditions.

The proposed communication system architecture, as illustrated in Fig. 1, is modular and scalable. It begins at the groundwater quality monitoring station, where key electrical parameters—such as voltage and current from the solar photovoltaic (PV) array and the supplementary electrical grid—are continuously measured using appropriate sensors and microcontroller-based data acquisition units. These data, along with water quality indicators (e.g., turbidity, pH, and conductivity), are encapsulated into structured payloads following the LoRaWAN data format standard [19].

The payloads are then transmitted wirelessly using a LoRa (Long Range) IoT module configured to operate in the 923.2 MHz ISM band with a channel bandwidth of 125 kHz. The use of LoRa technology ensures low-power, long-range communication with high resistance to interference, which is essential for remote or underground deployment where cellular coverage is limited or unreliable.

Upon transmission, the data packets are received by a strategically positioned LoRa IoT gateway, which serves as a relay between the end device (sensor node) and the cloud-based infrastructure. The gateway forwards the packets to a LoRa Network Server, which handles device authentication, packet de-duplication, and MAC layer management. From there, the data is routed to the LoRa Application Server, which processes and stores the information for visualization, decision-making, and system diagnostics. The backend system can also support remote device management functions such as firmware updates, transmission parameter optimization, and real-time alert generation.

This research not only validates the physical-layer feasibility of the communication system through experimental trials but also contributes to the development of a sustainable and intelligent environmental monitoring framework. The integration of energy harvesting (via solar cells), microgrid power management, and long-range IoT communication presents a viable solution for autonomous

and scalable deployment in smart agriculture, water resource management, and rural electrification initiatives.

2. Literature Review

The increasing demand for real-time data acquisition in environmental monitoring and energy management has intensified the role of Internet of Things (IoT) technologies across multiple domains. Among the wide spectrum of wireless communication protocols, Low-Power Wide-Area Network (LPWAN) technologies have emerged as the most promising due to their ability to provide long-range coverage with low energy consumption, minimal infrastructure cost, and scalability across diverse applications [1], [2]. Within this domain, LoRa (Long Range) technology has gained considerable attention as a flexible and robust solution, combining chirp spread spectrum (CSS) modulation with sub-GHz frequency operation to achieve communication over distances of several kilometers while operating at ultra-low power levels [3], [12-13].

2.1 LoRa and LPWAN in IoT Applications

LoRa operates in unlicensed ISM bands (e.g., 433 MHz, 868 MHz, and 923 MHz) and is distinguished from other LPWAN protocols such as NB-IoT and Sigfox by its adaptive data rate, high receiver sensitivity, and ability to balance range with throughput [2], [12]. Studies by Centenaro et al. [1] and Augustin et al. [3] highlight LoRa's superiority in scenarios requiring both coverage and longevity, particularly for smart city and industrial automation deployments. Unlike cellular-based NB-IoT, which relies on telecom infrastructure and incurs subscription costs, LoRa networks can be independently deployed, making them more adaptable to localized applications such as rural water quality monitoring and microgrid management [2].

2.2 Communication Requirements for Smart Grids

Smart grids require reliable and secure communication infrastructures to support real-time data exchange between distributed energy resources, demand response systems, and monitoring devices. Traditional wireless protocols such as Wi-Fi and ZigBee provide higher data rates but are constrained by limited coverage and higher energy demands [15-16]. In contrast, LoRa offers extended coverage and resilience to interference, making it a suitable candidate for remote grid nodes and distributed monitoring stations [17-18].

Giordano et al. [4] and Farhangi [15] stressed that smart grids depend on low bandwidth but highly reliable data channels for applications such as smart metering, energy usage profiling, and fault detection. Usman and Shami [17] further observed that the evolution of communication technologies for smart grids must strike a balance between latency tolerance and energy efficiency. In this context, LoRa's low duty cycle and minimal energy consumption per transmission are ideal for long-term autonomous deployments. Recent advances in LoRaWAN specification [7] have further enhanced its suitability by introducing security features, adaptive data rate (ADR), and support for bi-directional communication.

Adelantado et al. [12] and Bor et al. [14] critically assessed the scalability of LoRaWAN networks, emphasizing challenges such as interference, duty-cycle limitations, and network congestion in dense deployments. However, their findings confirmed that with appropriate spreading factors (SF) configurations and gateway placement, LoRa systems can support thousands of end devices with acceptable packet delivery ratios. These characteristics make LoRa particularly relevant for micro smart grid and environmental monitoring applications, where robust, energy-efficient communication is essential.

2.3 IoT in Environmental and Water Quality Monitoring

Environmental monitoring has been one of the earliest application domains where LoRa has demonstrated its potential. Raza et al. [13] outlined LPWAN's role in low-data-rate applications such as air quality monitoring, agricultural soil sensing, and water quality assessment, where frequent but lightweight data packets must be transmitted reliably over long distances.

For water quality applications, IoT-enabled sensors measuring pH, turbidity, dissolved oxygen, and conductivity play a crucial role in detecting pollution, monitoring freshwater resources, and supporting disaster prevention measures. Conventional systems often rely on GSM or wired networks, which limit deployment flexibility and increase operational costs. LoRa-based systems overcome these limitations by offering real-time data acquisition in rural or infrastructure-limited regions. Khonrang et al. [24] demonstrated the feasibility of LoRa-based wildfire and environmental sensors using multi-hop mesh architectures, highlighting how long-range communication can support environmental protection in difficult terrains.

Recent works, such as those by Benzi et al. [18], explored smart metering and household electricity monitoring, showing parallels with environmental monitoring in terms of low-bandwidth data requirements. Both applications benefit from LoRa's robustness in non-line-of-sight environments, especially when sensor nodes are deployed at low heights where Fresnel zone obstructions and multipath fading become significant [22-23].

2.4 Propagation Modeling and Link Budget Considerations

Accurate prediction of wireless performance in real deployments requires careful propagation modeling. Classical models such as Free-Space Path Loss (FSPL) [9-10] provide a baseline but often underestimate attenuation in near-ground IoT applications due to multipath effects, diffraction, and ground reflections. Studies by Adelantado et al. [12] and Bor et al. [14] reported significant discrepancies between FSPL predictions and real-world LoRa measurements, especially in rural and obstructed areas.

The Fresnel zone analysis remains critical for ensuring link reliability. Obstruction of more than 40% of the first Fresnel zone can lead to severe signal degradation [22]. Research by Viratikul et al. [23] in underwater IoT environments demonstrated similar attenuation challenges, emphasizing the importance of optimizing antenna height and placement. These findings are consistent with the results of the present study, where a 35 dB deviation between simulated FSPL and measured RSSI was attributed to Fresnel obstruction, multipath fading, and environmental losses.

2.5 LoRa for Energy-Constrained Systems and Microgrids

Energy efficiency is a recurring theme in IoT research, particularly for battery- or solar-powered nodes. Usman and Shami [17] and Hassan et al. [5] highlighted the necessity of communication protocols that minimize energy per bit transmitted. LoRa's low duty cycle and short time-on-air (ToA) address this requirement effectively. In the context of micro smart grids, where sensor nodes monitor both environmental parameters and electrical variables, LoRa provides the dual advantage of low-power operation and sufficient reliability for decision-making tasks.

Integration of renewable-powered IoT systems with microgrids has been investigated in several recent works. Khonrang et al. [25] developed a microgrid power supply for seismic sensors, demonstrating how autonomous energy management can be combined with IoT communication for continuous monitoring. Similarly, Viratikul et al. [26] studied the electromagnetic properties of biological media, contributing to the broader understanding of how IoT and smart grids can support scientific and medical monitoring. These contributions underscore the multidisciplinary applicability of LoRa-based communication systems.

2.6 Identified Gaps and Research Contribution

While existing studies confirm the effectiveness of LoRa in smart grid and environmental applications, several challenges remain unresolved:

- Propagation Uncertainty – Most prior works rely on FSPL or empirical models without addressing the discrepancy between theory and practice in near-ground rural deployments [9], [12], [14].
- Energy Autonomy – Although LoRa enables low-power operation, few studies explore the integration of LoRa nodes with solar-powered microgrids, which can ensure long-term sustainability [25].
- Application-Specific Optimization – Existing research often focuses on general IoT applications. Tailored solutions for water quality monitoring stations integrated with micro smart grids remain limited.
- Latency and Throughput Analysis – While packet delivery ratio is widely studied, comprehensive evaluation of latency, time-on-air, and effective throughput under real conditions has not been adequately addressed [18].

3. Free-Space Path Loss and Link Budget Analysis

3.1 Free-Space Path Loss for LoRa

This section presents the theoretical modeling and calculation of the Free-Space Path Loss (FSPL) and link budget for the proposed LoRa-based communication system. The FSPL model is adopted as the primary analytical tool due to its suitability for line-of-sight (LoS) environments, which characterize the current deployment scenario—an open and unobstructed communication path between the transmitter and receiver. Such conditions are commonly encountered in above-ground monitoring installations or where sensor nodes are elevated on poles or placed on rooftops to ensure minimal obstruction.

Operating in the 900 MHz ISM band, specifically at 923.2 MHz, the LoRa communication system is relatively resilient to environmental losses such as rain attenuation and foliage scattering, which tend to become more significant at higher frequencies (e.g., in the GHz range). However, for completeness, it is acknowledged that such factors could introduce marginal degradation to signal strength in long-range or dense deployments. For the purposes of this model, these impairments are assumed negligible, and the FSPL model is applied as a baseline reference under ideal propagation conditions [8-10].

To rigorously evaluate the communication link, both the free-space path loss and the link budget are calculated using standardized system parameters including transmitter power, receiver sensitivity, antenna gains, and operating frequency. These calculations provide theoretical estimates of signal attenuation, maximum communication range, and expected RSSI values, which are later compared to empirical measurements obtained from the field deployment.

$$FSPL = 20 \log_{10}(d) + 20 \log_{10}(f) + 20 \log_{10}\left(\frac{4\pi}{c}\right) - G_{Tx} - G_{Rx} \quad (1)$$

d is the distance linking the antennas; f denotes the transmitting frequency. G_{Tx} is the gain of the transmitting antenna, while G_{Rx} represents the gain of the receiving antenna, and c is the speed of light in a vacuum (meters per second).

The link budget, which estimates the received signal power at the receiver, is calculated as equation (2) [21], [27].

$$P_{Rx} = P_{Tx} + G_{Tx} + G_{Rx} - FSPL \quad (2)$$

The design framework and analytical calculations in this study are grounded in the system parameters summarized in Table 1, which defines key elements such as the operating frequency, transmission power, antenna gains, and assumed losses. As depicted in Fig. 2, the communication channel model represents a direct line-of-sight (LoS) wireless link between a remote groundwater monitoring node and a central IoT gateway. Given the absence of physical obstructions, the Free-Space Path Loss (FSPL) model is deemed appropriate for estimating signal attenuation over distance.

Utilizing the parameters outlined in Table 1, the FSPL was computed using the standard logarithmic model. Over a 2 km transmission distance at an operating frequency of 923.2 MHz, the path loss was found to be 97.76 dB, which reflects the theoretical signal degradation due to free-space propagation. This value provides a baseline for assessing the link performance and plays a critical role in evaluating the overall system feasibility.

Table 1 Parameters used in the link budget and free-space path loss (FSPL) analysis.

Parameter	Value	Unit
Transmission frequency (f)	923.2	MHz
Distance between nodes (d)	2	km
Transmit power (P_{Tx}) (SX1276 Chip) [6]	14	dBm
Transmit antenna gain (G_{Tx})	3	dBi
Receive antenna gain (G_{Rx})	8	dBi
Tx antenna height	1	m
Rx antenna height	6	m
Bandwidth	125	kHz
Spreading factor (SF)	10	-
Modulation scheme	FHSS	-

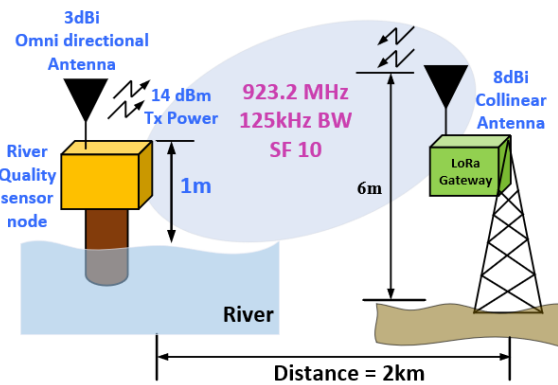


Fig. 2 Communication channel diagram illustrates the free-space path loss (FSPL) model between the transmitter and receiver under line-of-sight (LoS) conditions.

With this path loss, the link budget was calculated to estimate the received signal strength at the receiver. Considering a transmission power of 14 dBm, a transmit antenna gain of 3 dBi, and a receive antenna gain of 8 dBi, the resulting received signal strength was determined to be approximately -72.76 dBm. This value falls well within the acceptable sensitivity range of typical LoRa receivers and confirms the feasibility of reliable long-range communication for the intended application.

The calculated received power serves as a theoretical benchmark for subsequent experimental validation. In practice, environmental effects such as ground reflection, multipath propagation, and atmospheric conditions may influence the actual RSSI values [30]. Therefore, the comparison between theoretical predictions and real-world measurements provides critical insight into the accuracy of the model and guides further system optimization. This analysis is especially important in remote monitoring scenarios where power efficiency and communication reliability are paramount.

3.2 Fresnel Zone Analysis for LoRa

In wireless communication systems, particularly those operating over long distances such as LoRa (Long Range) networks, the Fresnel zone is a critical parameter influencing signal propagation and link reliability. The Fresnel zone represents an elliptical region around the line-of-sight (LoS) path between a transmitter and a receiver, within which obstacles can cause diffraction, phase shifting, and signal attenuation, thereby degrading communication performance [22].

For optimal signal strength and minimal interference, it is recommended that at least 60% of the first Fresnel zone remain free of obstructions. Any encroachment into this zone by terrain, foliage, buildings, or other structures can introduce non-line-of-sight propagation effects and increase the likelihood of signal fading or loss.

The radius of the first Fresnel zone at its widest point (midpoint between transmitter and receiver) can be calculated using the following equation (3) [23], [29].

$$F_1 = \sqrt{\frac{\lambda d_1 d_2}{d_1 + d_2}} \quad (3)$$

Where F_1 is Radius of the first Fresnel zone (meters), λ is wavelength of the signal (meters), d_1 and d_2 represent Distances from the obstacle to the transmitter and receiver respectively (meters).

For the proposed LoRa-based system operating at 923.2 MHz over a 2 km line-of-sight (LoS) link, the radius of the first Fresnel zone at the midpoint is calculated to be approximately 12.74 meters that show the Fresnel diagram in Fig.3.

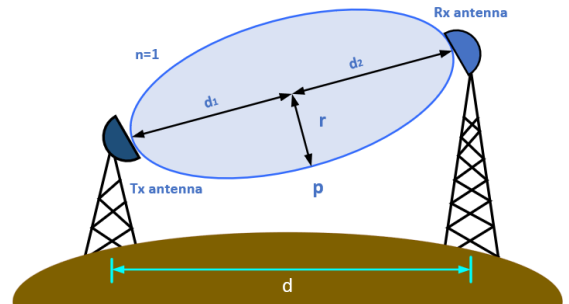


Fig. 3 Diagram of the Fresnel zone. d is the distance between the transmitter and the receiver; r is the radius of the first Fresnel zone ($n=1$) at point P . P is d_1 away from the transmitter, and d_2 away from the receiver.

Based on established design guidelines, it is generally recommended that at least 60% of the first Fresnel zone remains unobstructed, corresponding to a minimum clearance of 7.64 meters. Given the current antenna configuration—a transmit antenna height of 1 meter and a receive antenna height of 6 meters—the LoS path lies only 3.5 meters above the ground at the midpoint. This is well below the required clearance, suggesting that a substantial portion of the Fresnel zone may be obstructed. Such an obstruction can result in increased diffraction, reduced signal strength, and potentially degraded link reliability.

Despite this, empirical and theoretical evaluations of the link budget indicate that communication over a 2 km range is still feasible under the given conditions. With a transmit power of 14 dBm and LoRa modulation configured to Spreading Factor (SF) 10, the system benefits from increased receiver sensitivity and robustness against noise and interference. SF10 offers a good balance between range and data rate, enabling the receiver to successfully decode signals even in suboptimal propagation environments. Therefore, while the Fresnel zone obstruction may lead to some signal degradation, the system retains sufficient link margin to maintain reliable data transmission. Nevertheless, to further enhance communication reliability and reduce the risk of link outage, it is advisable to increase the transmit antenna height to improve Fresnel zone clearance and overall system performance.

4. Hardware Architecture of IoT-Based Water Quality Sensor Node.

4.1 LoRa water quality sensor node

This section presents the hardware architecture of the water quality sensor node, developed for remote environmental monitoring and data transmission using LoRa-based Internet of Things (IoT) communication technology [24], [28]. Sensor to operate autonomously in conjunction with a micro smart grid system, the sensor node enables real-time acquisition of environmental and electrical parameters and supports long-range, low-power wireless communication in remote or infrastructure-constrained settings.

At the core of the sensor node is the ATMEGA2560 microcontroller, an 8-bit low-power RISC-based processor chosen for its multiple digital and analog input/output channels, robust processing capability, and compatibility with embedded control and automation tasks. The microcontroller is programmed to manage the acquisition, processing, and transmission of data, orchestrating operations across both environmental and power monitoring subsystems.

The environmental sensing module comprises a suite of multi-parameter water quality sensors, which may include commercial or industrial-grade probes for measuring pH, electrical conductivity (EC), and dissolved oxygen (DO). These sensors communicate with the microcontroller using a combination of analog input ports and the RS-485 serial communication protocol, enabling flexible and scalable sensor integration. Through periodic sampling, the microcontroller collects and processes the raw signals into calibrated environmental data.

In addition to monitoring water quality, the microcontroller continuously tracks the power generation and consumption status of the integrated micro smart grid system, which typically includes a solar photovoltaic (PV) array, battery energy storage unit, and power conditioning devices such as charge controllers or grid-tied inverters. Critical electrical parameters, including voltage, current, and battery charge levels, are read via the analog-to-digital converter (ADC)

channels of the ATMEGA2560. These values are essential not only for maintaining the node’s operational autonomy but also for enabling system-level energy optimization and diagnostics.

Once all environmental and electrical parameters are acquired, the ATMEGA2560 consolidates the information into structured data packets, which are transmitted to the SX1276 LoRa transceiver module through the Serial Peripheral Interface (SPI). This LoRa module operates in the sub-GHz ISM band (923.2 MHz) and enables long-range wireless communication between the sensor node and a LoRa gateway, which subsequently relays the data to a cloud-based server for visualization, analytics, and decision-making.

The complete node architecture—including sensing components, power interface, microcontroller, and communication modules—is illustrated in Fig. 4, while the detailed circuit of the LoRa water quality sensor node designed in this research is presented in Fig. 5

4.2 The LoRa IoT Gateway

The LoRa IoT gateway functions as the central relay point in the proposed system, connecting distributed water quality sensor nodes to the cloud monitoring platform. In this study, the gateway is designed as a single-channel device operating at 923.2 MHz with a 125 kHz bandwidth. The communication interface is built around the Semtech SX1276 transceiver chip, which provides robust LoRa modulation and demodulation capabilities for reliable long-range wireless communication.

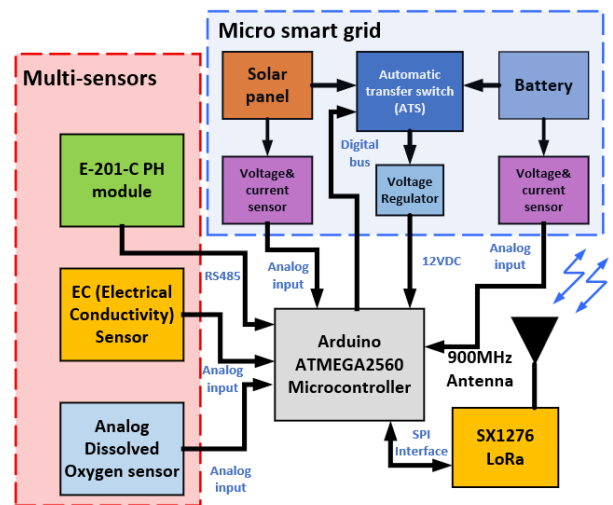


Fig. 4 Diagram of a water quality node sensor for research purposes.

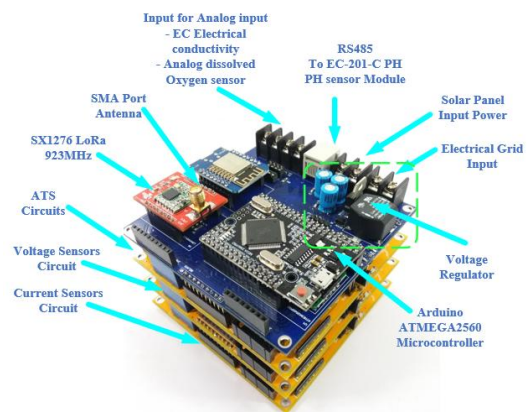


Fig. 5 LoRa water quality sensor node circuit designed in research.

At the system level, the gateway integrates an embedded Raspberry Pi 3 processor, which manages the operation of the SX1276 module, executes packet forwarding tasks, and provides network connectivity through Ethernet or Wi-Fi. Raspberry Pi 3 runs lightweight software to handle uplink packet reception, error checking, and forwarding of data to the LoRa Network Server (LNS). The LNS ensures device authentication, packet de-duplication, and adaptive data rate (ADR) management, maintaining secure and efficient communication across the network.

After processing at the LNS, data is forwarded to the LoRa Application Server, where it is structured for storage and visualization. In this implementation, the ThingSpeak cloud platform is employed as the application layer, providing customizable dashboards for real-time visualization of pH, electrical conductivity, dissolved oxygen, turbidity, temperature, and micro smart grid parameters. ThingSpeak also supports historical data storage, threshold-based alerts, and integration with decision-support tools for water quality management.

For reliable operation, the gateway is equipped with dual power sources: a conventional AC supply and a solar-powered backup system integrated with the micro smart grid. This hybrid energy management ensures continuous operation even during grid instability. Local buffering capability within the Raspberry Pi 3 allows temporary storage of sensor data if backhaul connectivity is lost, preventing data loss and ensuring seamless recovery once the link is restored.

As illustrated in Fig. 6, the LoRa IoT gateway comprises four main subsystems: the SX1276 single-channel concentrator, the Raspberry Pi 3 embedded processor, the network backhauls interface (Ethernet/Wi-Fi), and the power management unit. The data flow proceeds from water quality sensor nodes → LoRa gateway → LNS → Application Server → ThingSpeak dashboard, ensuring robust, scalable, and real-time environmental monitoring, while the detailed circuit design of the LoRa gateway implemented in this research is shown in Fig. 7.

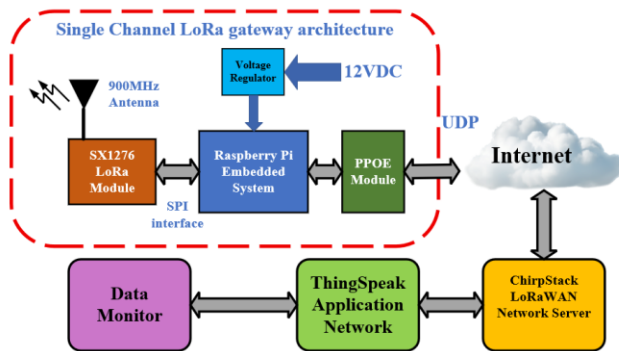


Fig. 6 LoRa gateway connectivity architecture.

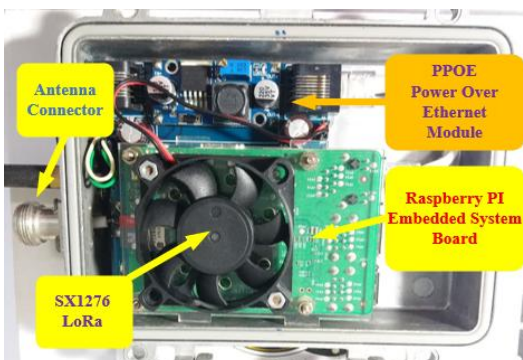


Fig. 7 LoRa gateway circuit designed in research.

5. Simulation and Experimental Results.

This section presents a detailed comparison between the simulated and experimental results of the proposed LoRa-based communication system. The objective is to evaluate the accuracy of the theoretical free-space path loss (FSPL) model and simulation outcomes against empirical measurements obtained from the field deployment. Such a comparison is critical for validating the design assumptions, identifying potential discrepancies, and highlighting the influence of real-world environmental conditions on system performance. In particular, this analysis enables researchers to determine how well simplified propagation models represent practical scenarios, assess the reliability of simulation-based predictions, and identify areas where system parameters such as antenna placement, channel bandwidth, or modulation scheme may require optimization to ensure consistent performance across diverse deployment environments.

5.1 FSPL Simulation and Measurement Results

The FSPL model was simulated using Keysight Advanced Design System (ADS) software to predict the expected signal behavior under ideal line-of-sight (LoS) conditions. Fig. 8 illustrates the simulated environment for the received signal strength indicator (RSSI), where the received power at the receiver was calculated to be approximately -72.77 dBm at a 2 km link distance. This result closely aligns with the theoretical value derived from the FSPL analytical model, confirming the internal consistency of the simulation framework.

In contrast, Fig. 9 presents the empirical measurements obtained during the field experiment. The RSSI was recorded at the receiver positioned 2 km away from the transmitter using a calibrated RF spectrum analyzer. A total of 20 independent measurements were performed under consistent test conditions, yielding an average received signal strength of -108 dBm. This measured value exhibits a substantial deviation of more than 35 dB compared to the simulated and theoretical predictions.

The observed discrepancy can be explained by several real-world propagation factors not incorporated into the idealized FSPL model. Key contributors include:

- 1) Ground Reflection and Multipath Fading – In near-ground deployments, reflections from the terrain and surrounding structures can lead to destructive interference at the receiver, significantly attenuating the effective signal strength.
- 2) Fresnel Zone Obstruction – As previously analyzed in Section 2.2, the first Fresnel zone clearance was not fully satisfied at the 2 km link distance, with the line-of-sight path only 3.5 m above the ground compared to the recommended minimum clearance of 7.64 m. This partial obstruction increases diffraction losses and reduces RSSI.
- 3) Atmospheric and Environmental Effects – Variations in humidity, temperature, and vegetation along the propagation path introduce additional attenuation mechanisms, particularly scattering and absorption, which are absent in the FSPL model.
- 4) Hardware and Implementation Losses – Practical factors such as antenna alignment errors, cable losses, and connector mismatches may further reduce the effective signal strength compared to the ideal simulation.

Despite the deviation, the measured RSSI of -108 dBm remains within the receiver sensitivity threshold of the SX1276 transceiver, enabling a packet delivery ratio (PDR) of approximately 95%, as observed in the experimental trials. This demonstrates that although the FSPL model overestimates the received power by neglecting real-world impairments, the system still achieves reliable communication performance under field conditions.

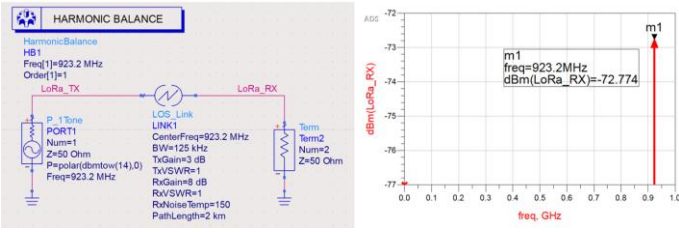


Fig. 8 the ADS simulation outcomes of the RSSI at the receiver.

$$ToA = \frac{Payload (bits)}{Bandwidth} \quad (5)$$

With a payload size of 30 bytes and a bandwidth of 125 kHz under FHSS modulation, the estimated time-on-air (ToA) for each packet was calculated according to equation (5) [11]. Assuming a bit rate of 50 kbps, the total transmission time for 240 bits of data is approximately 4.8 milliseconds per packet. This short ToA significantly reduces channel occupancy, lowers collision probability in multi-node scenarios, and minimizes the overall energy expenditure of each IoT device [31].

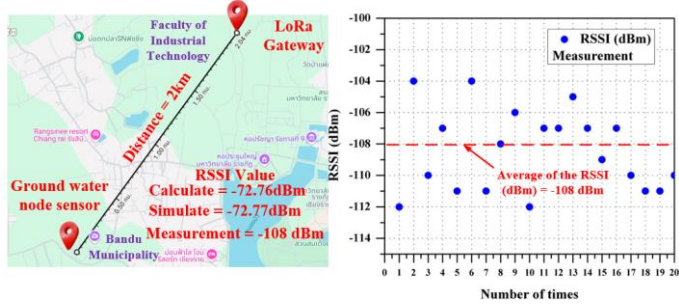


Fig. 9 Depicts the measurement results of the RSSI at 2 km.

The achieved balance between high packet delivery ratio (95%), low latency (~4.8 ms), and low energy consumption reinforces the viability of LoRa for long-range, energy-constrained monitoring systems. Importantly, these results confirm that the system can support frequent data transmissions while preserving both channel efficiency and network scalability. Such performance is particularly advantageous for applications requiring real-time environmental monitoring and smart grid diagnostics, where timely updates of water quality and electrical parameters are critical for informed decision-making.

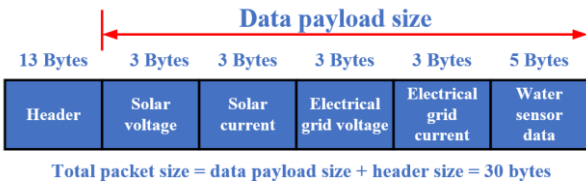


Fig. 10 The total data packets' payload size.

As shown in Fig. 11, the water quality monitoring station integrates a LoRa sensor node with a micro smart grid system, enabling autonomous operation powered by renewable energy. The node continuously measures environmental and electrical parameters, encapsulates the data into structured packets, and transmits them via the LoRa IoT gateway to the application server. The application layer—implemented using ThingSpeak in this research—facilitates real-time data visualization, historical trend analysis, and alert generation, providing stakeholders with a reliable platform for water resource management and microgrid operation.

This comparison underscores the importance of incorporating advanced propagation models (e.g., two-ray ground reflection or empirical path loss models such as Okumura-Hata) for more accurate prediction of system performance in near-ground, long-range IoT deployments. Future work may also investigate the impact of antenna height optimization and diversity schemes to mitigate multipath fading and improve link reliability.

5.3 Signal-to-Noise Ratio, Link Budget, and Throughput Analysis

5.2 Packet Delivery Analysis and Latency Considerations

To evaluate the reliability of the proposed LoRa-based communication system, a total of 100 data packets, each containing a payload of 30 bytes, were transmitted from the IoT sensor node to the LoRa gateway, as illustrated in Fig. 10. Out of these, 95 packets were successfully received, yielding a packet delivery ratio (PDR) of 95%, as calculated using equation (4). This level of reliability is particularly noteworthy given that the average measured RSSI was -108 dBm, which is close to the receiver sensitivity threshold of the SX1276 transceiver under frequency-hopping spread spectrum (FHSS) modulation. Despite operating near this limit, the system demonstrated stable performance with only minimal packet loss, highlighting the robustness of LoRa modulation for long-range communication in challenging environments.

In addition to packet delivery and latency evaluation, further performance characterization of the LoRa-based communication link was conducted by analyzing the signal-to-noise ratio (SNR), link budget, and achievable throughput. These metrics provide deeper insight into the robustness and efficiency of the proposed system under practical deployment conditions.

$$Packet\ Delivery\ Ratio = \left(\frac{Number\ of\ received\ packets}{Number\ of\ transmitted\ packets} \right) \times 100\% \quad (4)$$

Beyond packet delivery reliability, latency performance represents a critical metric for determining the suitability of LoRa technology in time-sensitive applications, such as environmental monitoring, micro smart grid control, and real-time decision-making. In the current implementation, the system operated with a transmit power of 14 dBm and a low duty cycle, thereby ensuring low energy consumption per transmission—an essential characteristic for remote deployments powered by solar panels or batteries [26].

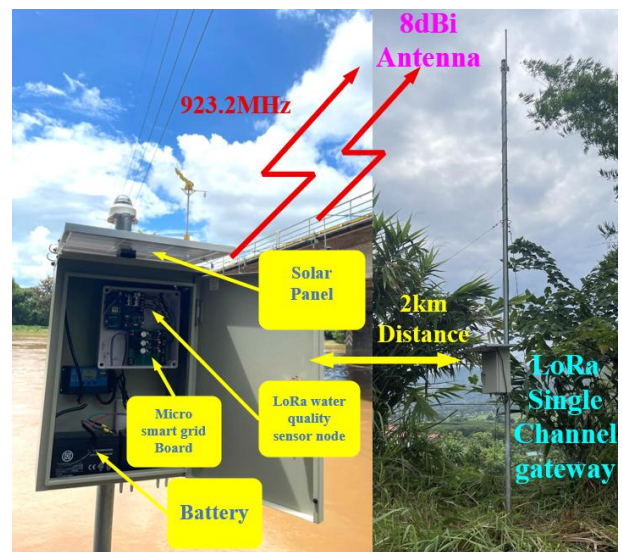


Fig. 11 The water quality monitoring station.

1) Signal-to-Noise Ratio (SNR)

Using a channel bandwidth of 125 kHz and an assumed receiver noise figure of 6 dB (typical for the SX1276 transceiver), the thermal noise floor was calculated as approximately -123 dBm, leading to a receiver noise floor of -117 dBm. With the experimentally measured received signal strength indicator (RSSI) of -108 dBm, the resulting SNR was estimated to be $+9$ dB. This value confirms that the received signal, although significantly attenuated compared to the FSPL prediction, remains above the minimum sensitivity threshold required for reliable demodulation under FHSS modulation.

2) Link Budget Analysis

The free-space path loss (FSPL) at 2 km for 923.2 MHz was calculated to be 97.76 dB, yielding a theoretical received power of -72.8 dBm when considering an effective isotropic radiated power (EIRP) of 17 dBm (14 dBm transmit power plus 3 dBi antenna gain) and an 8 dBi receive antenna. However, the measured RSSI of -108 dBm corresponds to an effective path loss of approximately 133 dB, indicating an additional attenuation of about 35 dB compared to the ideal FSPL model. This excess loss can be attributed to environmental factors such as ground reflection, Fresnel zone obstruction, and multipath fading.

To further assess link feasibility, the maximum allowable path loss (MAPL) was estimated for different SNR targets. With a receiver noise floor of -117 dBm:

- For a target SNR of 0 dB, the MAPL is approximately 142 dB.
- For a target SNR of 7 dB, the MAPL is 135 dB.
- For a target SNR of 10 dB, the MAPL is 132 dB.

Given that the measured path loss is 133 dB, the system performance lies between the 7 dB and 10 dB sensitivity margins, which aligns with the measured SNR of about $+9$ dB. This analysis confirms that despite additional attenuation, the link remains robust enough to support reliable communication.

3) Throughput Performance

Throughput analysis was performed using a payload size of 30 bytes (240 bits) and a bit rate of 50 kbps under FHSS modulation. The calculated time-on-air (ToA) for a single packet is approximately 4.8 ms, indicating efficient channel utilization with minimal occupancy. At the given bitrate, the instantaneous payload throughput corresponds to 50 kbps, while accounting for the measured packet delivery ratio (PDR) of 95%, the effective throughput is reduced slightly to 47.5 kbps.

This balance of high reliability (95% PDR), adequate SNR ($+9$ dB), and efficient throughput (47.5 kbps) demonstrates that the proposed LoRa-based system is well-suited for long-range, energy-constrained monitoring applications. By maintaining robust connectivity within the receiver sensitivity threshold, the system ensures timely and reliable data transmission for environmental monitoring and micro smart grid operations, even in scenarios where environmental losses exceed theoretical predictions. Moreover, the short ToA significantly reduces collision probability in multi-node networks, which is particularly important in dense deployments where multiple sensors share the same channel. This efficiency also translates into lower energy consumption per packet, thereby extending node lifetime in battery-powered or solar-assisted scenarios. In addition, the effective throughput achieved compares favorably with similar LoRa-based deployments reported in the literature, confirming the scalability and practicality of the proposed design for real-world IoT applications.

6. Discussion

The comparative analysis between theoretical models, simulations, and experimental measurements provides valuable insights into the strengths and limitations of LoRa-based communication for smart grid-integrated water quality monitoring. The divergence between the FSPL prediction (-72.8 dBm) and the measured RSSI (-108 dBm) illustrates the critical influence of real-world propagation impairments. Environmental factors such as Fresnel zone obstruction, multipath fading, and ground reflection increase attenuation beyond theoretical values. This outcome emphasizes that while FSPL provides a useful baseline, it cannot fully capture the complexity of near-ground IoT deployments. Similar findings are reported in [12], [14], where LoRa experiments demonstrated link performance degradation in obstructed rural and urban environments compared to free-space predictions.

The measured signal-to-noise ratio (SNR) of $+9$ dB is an important result, as it demonstrates the system's ability to operate reliably close to the receiver's sensitivity threshold. This is consistent with the maximum allowable path loss (MAPL) calculations, which indicated that the system remains functional within a range of 132–142 dB. The correlation between RSSI, SNR, and packet delivery ratio (PDR) confirms that the communication link is not only theoretically feasible but also resilient under practical conditions. In this study, the system achieved a 95% PDR, which is comparable to or better than reported results in related LoRa deployments for environmental monitoring [2], [13].

Latency and throughput analysis further strengthen the case for using LoRa in smart grid applications. With a time-on-air of 4.8 ms per 30-byte packet, the system maintains low latency while achieving an effective throughput of 47.5 kbps after accounting for PDR. This efficiency supports frequent updates without overloading the channel, a key requirement for applications such as real-time water quality tracking, microgrid diagnostics, and early-warning systems. Comparable research on LoRaWAN-based smart metering applications [15], [18] reported similar performance, confirming that LoRa can balance low energy consumption with sufficient data capacity for continuous monitoring.

Another important discussion point is energy efficiency. Since the sensor nodes are designed for battery and solar operation, minimizing energy use per transmission is critical. The combination of low duty cycle operation and short packet transmission time significantly reduces energy drain, extending node lifetime. This characteristic makes the system scalable for wider deployments where maintenance and battery replacement are costly. Moreover, the integration with a micro smart grid not only supports power resilience for the gateway but also provides a framework for energy harvesting and load management, bridging environmental monitoring with sustainable power systems.

Finally, the results suggest practical strategies for improvement. Antenna elevation and diversity techniques could mitigate Fresnel zone losses, while adaptive data rate (ADR) and forward error correction (FEC) could enhance reliability in noisy environments. Future enhancements such as multi-hop routing or repeater nodes may extend coverage beyond 2 km, aligning with large-scale deployments. By combining these improvements with the demonstrated robustness of LoRa, the system has strong potential as a cost-effective and sustainable solution for both environmental sensing and smart grid communication.

7. Conclusion

This study presented the design and performance evaluation of a LoRa-based data transmission system for water quality monitoring stations integrated with micro smart grid technology. The system was developed to support autonomous, energy-efficient, and long-range communication in remote or infrastructure-limited environments where conventional wired or cellular solutions are either impractical or costly.

Theoretical modeling using the free-space path loss (FSPL) framework and simulation in Keysight ADS predicted reliable communication at a 2 km link distance with a received signal strength of approximately -72.8 dBm. However, experimental field trials revealed an average RSSI of -108 dBm, reflecting an additional attenuation of about 35 dB due to environmental effects such as Fresnel zone obstruction, multipath fading, and ground reflection. Despite this discrepancy, the system maintained a packet delivery ratio (PDR) of 95%, demonstrating the robustness of LoRa modulation even under near-threshold operating conditions.

Further analysis confirmed that the measured signal-to-noise ratio (SNR) of +9 dB aligns with the system's link budget and maximum allowable path loss, ensuring reliable communication within the receiver sensitivity limits. The measured time-on-air (ToA) of 4.8 ms per 30-byte packet and the effective throughput of 47.5 kbps highlighted the system's capability to support frequent transmissions with minimal latency and low energy consumption, making it suitable for long-term battery- and solar-powered deployments.

Beyond technical validation, this research also demonstrates the potential of LoRa-enabled smart grid integration to deliver dual benefits: real-time environmental monitoring and enhanced energy resilience through renewable-powered nodes. Such integration not only reduces operational costs but also supports sustainability goals by enabling intelligent water management, efficient load control, and early fault detection in distributed microgrid infrastructures.

The outcomes confirm that the proposed design is a practical, scalable, and sustainable solution for long-range IoT deployments in both rural and urban settings. Looking forward, future work will focus on extending the system with multi-hop routing, antenna height optimization, and adaptive data rate schemes to improve coverage and resilience in obstructed or high-interference environments. Additionally, the incorporation of advanced propagation models, multi-channel gateways, and machine learning-based network optimization is expected to further enhance prediction accuracy, scalability, and adaptability across diverse deployment scenarios.

Acknowledgements

The success of this research was under the support and the assistance from Thailand Science Research and Innovation and Chiang Rai Rajabhat University, Project code FF67-1-007.

References

- [1] Centenaro, M., Vangelista, L., Zanella, A. and Zorzi, M., Long-range communications in unlicensed bands: the rising stars in the IoT and smart city scenarios. *IEEE Wireless Communications*. 23 (2016) 60-67, doi: <https://doi.org/10.1109/MWC.2016.7721743>.
- [2] Sinha, R. S., Wei, Y. and Hwang, S.-H., A survey on LPWA technology: LoRa and NB-IoT. *ICT Express*. 3 (2017) 14-21, doi: <https://doi.org/10.1016/j.icte.2017.03.004>.
- [3] Augustin, A., Yi, J., Clausen, T. H. and Townsley, W., A Study of LoRa: Long Range & Low Power Networks for the Internet of Things. *Sensors*. 16 (2016) 1466, doi: <https://doi.org/10.3390/s16091466>.
- [4] Giordano, V., Fulli, R. and Sánchez Jiménez, A. *Smart Grid Projects Outlook 2017: Facts, Figures and Trends in Europe*. EUR 28942 EN, Publications Office of the European Union, Luxembourg, (2018) 1-136, doi: <https://doi.org/10.2760/701587>.
- [5] Hu, J., Zhu J. and Platt, G. Smart grid — The next generation electricity grid with power flow optimization and high power quality. in *2011 International Conference on Electrical Machines and Systems*. (2011) 1-6, doi: <https://doi.org/10.1109/ICEMS.2011.6073433>.
- [6] Semtech Corporation. *SX1276/77/78/79 – 137 MHz to 1020 MHz Low Power Long Range Transceiver Datasheet*. Rev. 5, Semtech Corporation, Camarillo, CA, (2017) 1-132, <<https://www.semtech.com/products/wireless-rf/lora-core/sx1276>>.
- [7] LoRa Alliance. *LoRaWAN 1.1 Specification*. Ver. 1.1, LoRa Alliance, Fremont, CA, (2017) 1-103, <<https://lora-alliance.org>>.
- [8] Keysight Technologies. *Keysight Advanced Design System (ADS) – RF and Microwave Design Software*. Ver. 2022, Keysight Technologies Inc., Santa Rosa, CA, (2022) 1-2458, <<https://www.keysight.com>>.
- [9] T. Rappaport. *Wireless Communications: Principles and Practice*. 2nd edn., Prentice Hall, 2002.
- [10] A. Goldsmith. *Wireless Communications*, Cambridge Univ. Press, 2005, doi: <https://doi.org/10.1017/CBO9780511841224>.
- [11] Gozalvez, J., New 3GPP Standard for IoT [Mobile Radio]. *IEEE Vehicular Technology Magazine*. 11 (2016) 14-20, doi: <https://doi.org/10.1109/MVT.2015.2512358>.
- [12] Adelantado, F., Vilajosana, X., Tuset-Peiro, P., Martinez, B., Melia-Segui, J. and Watteyne, T., Understanding the Limits of LoRaWAN. *IEEE Communications Magazine*. 55 (2017) 34-40, doi: <https://doi.org/10.1109/MCOM.2017.1600613>.
- [13] Raza, U., Kulkarni, P. and Sooriyabandara, M., Low Power Wide Area Networks: An Overview. *IEEE Communications Surveys & Tutorials*. 19 (2017) 855-873, doi: <https://doi.org/10.1109/COMST.2017.2652320>.
- [14] Bor, M. C., Roedig, U., Voigt, T. and Alonso, J. M. Do LoRa low-power wide-area networks scale? in *the 19th ACM International Conference on Modeling, Analysis and Simulation of Wireless and Mobile Systems*. (2016), 59–67, doi: <https://doi.org/10.1145/2988287.2989163>.
- [15] Farhangi, H., The path of the smart grid. *IEEE Power and Energy Magazine*. 8 (2010) 18-28, doi: <https://doi.org/10.1109/MPE.2009.934876>.
- [16] Fan, Z., Kulkarni, P., Gormus, S., Efthymiou, C., Kalogridis, G., Sooriyabandara, M., Zhu, Z., Lambbotharan, S. and Chin, W. H., Smart Grid Communications: Overview of Research Challenges, Solutions, and Standardization Activities. *IEEE Communications Surveys & Tutorials*. 15 (2013) 21-38, doi: <https://doi.org/10.1109/SURV.2011.122211.00021>.
- [17] Usman, A. and Shami, S. H., Evolution of Communication Technologies for Smart Grid applications. *Renewable and Sustainable Energy Reviews*. 19 (2013) 191-199, doi: <https://doi.org/10.1016/j.rser.2012.11.002>.

- [18] Benzi, F., Anglani, N., Bassi, E. and Frosini, L., Electricity Smart Meters Interfacing the Households. *IEEE Transactions on Industrial Electronics*. 58 (2011) 4487-4494, doi: <https://doi.org/10.1109/TIE.2011.2107713>.
- [19] J. Haapola, Z. Shelby, C. Pomalaza-Raez and P. Mahonen. Low power wireless sensor networks: Survey of MAC and routing protocols. in *14th International Conference on Computer Communications and Networks (ICCCN)*. (2005), 20-27, doi: <https://doi.org/10.1109/ICCCN.2005.1523780>.
- [20] Kalogridis, G., Efthymiou, C., Denic, S. Z., Lewis, T. A. and Cepeda, R. Privacy for Smart Meters: Towards Undetectable Appliance Load Signatures. in *2010 First IEEE International Conference on Smart Grid Communications*. (2010), 232-237, doi: <https://doi.org/10.1109/SMARTGRID.2010.5622047>.
- [21] Boonlom, K., Chomtong, P., Zhang, W., Amsdon, T. J., Oberhammer, J., Robertson, I. D. and Somjit, N., Advanced Studies on Optical Wireless Communications for in-Pipe Environments: Bandwidth Exploration and Thermal Management. *IEEE Access*. 12 (2024) 80607-80632.
- [22] Boonlom, K., Chudpooti, N., Rungraungsilp, S., Zhang, W., Amsdon, T., Oberhammer, J. and Somjit, N., Multiwavelength Optical Sensing of Water-Level Stratification in Closed Plastic Pipelines Using Signal Attenuation and CIR Analysis. *IEEE Sensors Journal*. 25(2025) 35991-36001, doi: <https://doi.org/10.1109/JSEN.2025.3598923>.
- [23] Viratikul, R., Boonlom, K., Robertson, I., Amsdon, T., Janpugdee, P. and Somjit, N. Design and Evaluation of Optical Wireless Communication Systems for Underwater IoT Applications. in *2024 11th International Conference on Wireless Networks and Mobile Communications (WINCOM)*. (2024), 1-6, doi: <https://doi.org/10.1109/WINCOM62286.2024.10655875>.
- [24] Khonrang, J., Somphruek, M., Duangnakhorn, P., Siri, A. and Boonlom, K., Experimental and Case studies of Longdistance Multi-hopping Data Transmission Techniques for Wildfire Sensors Using the LoRa-Based Mesh Sensor Network. *International Journal of Electronics and Telecommunications*. 69 (2023) 419-424, doi: <https://doi.org/10.24425/ijet.2023.144378>.
- [25] Khonrang, J., Boonlom, K., Siri, A. and Klinhnu, J., *The Design and Development of Micro Grid Electrical Power Supply for Seismo Sensor with An Artificial Perceptron Neural Network*. 11 (2021) 2711-2721, doi: <https://doi.org/10.48047/rigeo.11.09.238>.
- [26] Viratikul, R., Boonlom, K., Mancinelli, E., Amsdon, T., Chudpooti, N., Hartley, U. W., Robertson, I., Pensabene, V., Oberhammer, J. and Somjit, N. Electromagnetic Property Characterization and Sensing of Endothelial Cells Growth Medium and Dulbecco's Phosphate Buffered Saline Solution for in vitro Cell Culture. in *2022 19th International Conference on Electrical Engineering/Electronics, Computer, Telecommunications and Information Technology (ECTI-CON)*. (2022), 1-4, doi: <https://doi.org/10.1109/ECTI-CON54298.2022.9795438>.
- [27] Boonlom, K., Viratikul, R., Robertson, I. D., Amsdon, T., Chudpooti, N. and Somjit, N. Illumination and Bandwidth Control Circuit for LED Optical Wireless Transmitter Driver Integrated with Passive Second-Order Equaliser for Pipe Robot Application. in *2023 Research, Invention, and Innovation Congress: Innovative Electricals and Electronics (RI2C)*. (2023), 1-5, doi: <https://doi.org/10.1109/RI2C60382.2023.10356036>.
- [28] Boonlom, K., Viratikul, R., Khonrang, J., Amsdon, T., Chudpooti, N., Rungraungsilp, S., Robertson, I., Janpugdee, P. and Somjit, N. Optimization of Heatsink Design for Enhanced Thermal Management in LED-Based Optical Wireless Communication Systems for In-Pipe Inspection Robots. in *2024 Research, Invention, and Innovation Congress: Innovative Electricals and Electronics (RI2C)*. (2024), 310-315, doi: <https://doi.org/10.1109/RI2C64012.2024.10784399>.
- [29] Boonlom, K., Viratikul, R., Janpugdee, P., Konpang, J., Chudpooti, N., Robertson, I., Amsdon, T. and Somjit, N. Active Pre-Equalizer for Broadband Optical Wireless Communication Integrated with RF Amplifier. in *2022 Research, Invention, and Innovation Congress: Innovative Electricals and Electronics (RI2C)*. (2022), 251-254, doi: <https://doi.org/10.1109/RI2C56397.2022.9910315>.
- [30] Rungraungsilp, S., Boonlom, K., Robertson, I., Somjit, N. and Morris, K. Implement an acoustic sound system by Hann Window with Fast Fourier Transform (FFT) to analyze characteristics in a pipe for robotic. in *2025 13th International Electrical Engineering Congress (iEECON)*. (2025), 1-4, doi: <https://doi.org/10.1109/iEECON64081.2025.10987830>.
- [31] Nie, X., Boonlom, K., Ma, C., Cheng, L., Roberston, I. D. and Qing, A. An Accurate Imaging Algorithm with Dual-Path Propagation Loss for Monostatic System. in *2023 IEEE International Symposium on Antennas and Propagation and USNC-URSI Radio Science Meeting (USNC-URSI)*. (2023), 471-472, doi: <https://doi.org/10.1109/USNC-URSI52151.2023.10238102>.